Leading-particle spectrum and impact-parameter distributions at very high energies

Jorge Dias de Deus
Centro de Física da Matéria Condensada, Instituto Nacional de Investigacão Científica, Av. Prof. Gama Pinto 2, 1699 Lisboa Codex, Portugal
(Received 22 March 1985)

With the assumption that the available energy for particle production in very-high-energy collisions is related to the impact-parameter inelastic overlap function it is shown that the shape in x of the leading-proton spectrum is strongly correlated with the shape in b of the overlap function. Changes with energy in the ratio $\sigma_{\text{elastic}}/\sigma_{\text{total}}$ will be reflected in changes in the leading-particle spectrum.

For the impact-parameter description of high-energy scattering it has always been difficult to include longitudinal distributions. However, recently, Chou, Yang, and Yen[1] made the observation that the pseudorapidity distribution at the CERN SPS $p\bar{p}$ collider[2] can be related to the collision impact parameter. From their calculation and fit to the data it turns out that the available energy E_A for particle production in the central region is a monotonic decreasing function of the impact parameter b.

This result is very suggestive. If the overlap between the incoming Lorentz-contracted extended hadrons is large, $b \simeq 0$, the available energy for particle production is large. On the contrary, if a collision is peripheral the hadrons go easily through each other and not much energy is left for particle production.

Here, following this intuitive picture, I propose a simple ansatz for the relation between the impact parameter b and the available energy fraction h_A, namely,

$$h_A = G(\tilde{b}^2, s) , \tag{1}$$

where $h_A \equiv 2E_A/\sqrt{s}$ is the available energy fraction for particle production in one hemisphere, $G(\tilde{b}^2,s)$ is the inelastic overlap function, $\tilde{b}^2 \equiv b^2/\sigma$ is the scaled impact-parameter variable, and σ is the inelastic cross section. One should notice that as $b \to 0$, $G \simeq 1$ and $h_A \simeq 1$, and as $b \to \infty$, $G \to 0$ and $h_A \to 0$, as required in the impact-parameter picture. One should further remark that with (1) the positivity and unitarity constraints on the overlap function, $0 \le G \le 1$, are translated into the bounds imposed on the available energy fractions, $1 \ge h_A \ge 0$.

The available energy fraction h_A is, by energy conservation, related to the energy fraction x_L retained by the jet of leading particles:

$$h_A + x_L = 1 . \tag{2}$$

Making use of (1) and (2) we can relate the inelastic overlap function to the leading-particle spectrum.

From (1) and (2) we have

$$\frac{1}{\sigma}\frac{d\sigma}{db^2} = \frac{\pi}{\sigma} G(\tilde{b}^2,s) = \frac{1}{\sigma}\frac{d\sigma}{dx_L}\frac{dx_L}{db^2} \tag{3}$$

and

$$\frac{1}{\sigma}\frac{d\sigma}{dx_L} = -\frac{\pi}{d\ln G/d\tilde{b}^2} \equiv -\frac{\pi}{(\ln G)'} . \tag{4}$$

For the variation of the leading spectrum with x_L one obtains

$$\frac{d}{dx_L}\left[\frac{1}{\sigma}\frac{d\sigma}{dx_L}\right] = -\frac{\pi}{G'}\frac{(\ln G)''}{(\ln G)'^2} . \tag{5}$$

From (4) the positivity of $d\sigma/dx_L$ is guaranteed by the decrease of G with b^2 (experimentally observed and expected in impact-parameter models). From (5) one sees that the x_L dependence of $d\sigma/dx_L$ is critically determined by the second logarithmic derivative of G. In Table I are listed some typical impact-parameter leading-particle distribution transforms.

The overlap functions in Table I are qualitatively not very different from each other, with all having $(\ln G)' < 0$ as observed in all elastic-scattering high-energy processes. However, because of the value of $(\ln G)''$, $=0$ in case (a), <0 in case (b), and >0 in case (c), they correspond to very different leading-particle spectra: constant $d\sigma/dx_L$ for the Gaussian overlap function, case (a), a decreasing leading-particle distribution for case (b), and a distribution increasing with x_L for case (c).

TABLE I. Examples of overlap functions and leading-particle distributions related by (5). The normalizations for the overlap functions and leading spectra are $(\pi/\sigma)\int G\,db^2 = 1$ and $(1/\sigma)\int (d\sigma/dx_L)dx_L = 1$, respectively. In case (b) the positive constants A and C are related: $A = \pi(1+C)\ln(1+1/C)$. In the limit $C \to \infty$ case (b) becomes case (a).

Overlap function		Leading spectrum	
$\frac{1}{\pi}\frac{d\sigma}{db^2} \equiv G(\tilde{b}^2)$		$\frac{1}{\sigma}\frac{d\sigma}{dx_L}$	$\langle x_L \rangle$
(a)	$e^{-\pi\tilde{b}^2}$	1	$\frac{1}{2}$
(b)	$\frac{C+1}{Ce^{A\tilde{b}^2}+1}$	$\frac{\pi}{A}\frac{C+1}{C+x_L}$	$\frac{1-C\ln(1+1/C)}{\ln(1+1/C)} < \frac{1}{2}$
(c)	$e^{-(2\pi\tilde{b}^2)^{1/2}}$	$-\ln(1-x_L)$	$\frac{3}{4}$

The question one may now ask is what constraints coming from the impact parameter should be imposed on the leading-particle spectrum. In first approximation the Gaussian overlap function is acceptable and the corresponding flat leading-particle spectrum gives also a fairly good description of the leading-proton-spectrum data. A more detailed impact-parameter analysis at CERN ISR energies reveals two important deviations from the Gaussian overlap function. At small b^2 there is a well-known flattening of the distribution. At large b^2 the behavior is of the type $\exp(-\lambda b)$ instead of $\exp(-\lambda b^2)$ (Ref. 3). The $\exp(-\lambda b)$ behavior at large b^2 is in fact expected to occur on rigorous grounds.[4] The consequences of these observations are, from cases (b) and (c) in Table I, quite obvious: relative to the flat distribution the leading spectrum will decrease with x at $x_L \simeq 0$ and will increase strongly at $x_L \simeq 1$. And this is precisely what is observed in the leading-proton spectrum (see Fig. 1).

A parametrization of the inelastic overlap function containing the required features just mentioned, but not pretending to be fully realistic, is the following:

$$G(\tilde{b}^2)=(1-d)\frac{C+1}{Ce^{A\tilde{b}^2}+1}+de^{-(2\pi\tilde{b}^2)^{1/2}} \tag{6}$$

with $0 \le d \le 1$. For the leading-particle spectrum one obtains

$$\frac{1}{\sigma}d\sigma/dx_L=(1-d)\frac{\pi}{A}\frac{C+1}{C+x_L}-d\ln(1-x_L)\ . \tag{7}$$

With $C=1$ ($A=4.36$) and $d=0.2$, for ISR energies, Eq. (6) gives $\sigma_{\rm el}/\sigma_{\rm tot}\simeq 0.17$ (experiment: 0.17—0.18) and from Eq. (7) the curve shown in Fig. 1 is obtained, corresponding to $\langle x_L \rangle \simeq 0.50$ (experiment: $\simeq 0.5$). The cross section associated to the $x_L \to 1$ diffractive peak is $\sigma_d = d \times \sigma \simeq 7$ mb (experiment: 7—8 mb).

To the extent that geometrical scaling in the impact parameter variable b^2/σ is satisfied the leading-particle spectrum should remain the same independent of energy. However, at the SPS $p\bar{p}$ collider, $\sqrt{s} \simeq 540$ GeV, the UA4 collaboration[6] found a 20% increase in the $\sigma_{\rm el}/\sigma_{\rm tot}$ ratio which corresponds to an appreciable blackening of the impact-parameter distribution. The blackening of the overlap function is, on the other hand, predicted in various models of high-energy scattering.[7] Such an effect in the present framework is achieved by decreasing C in Eq. (6) (a change in d is not effective and was not experimentally observed)[8] and naturally it amounts to modifying the leading-particle spectrum. In Fig. 2 I present curves for the overlap function and the leading-particle spectrum for different values of the $\sigma_{\rm el}/\sigma_{\rm tot}$ ratio. These predicted overlap-function leading-particle-spectrum correlations may be tested in future higher-energy experiments.

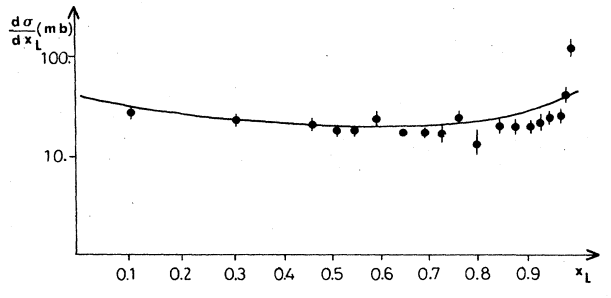

FIG. 1. Comparison of the curve (7) with ISR data (Ref. 5) on the leading-proton spectrum. The parameters were adjusted in order to obtain $\sigma_{\rm el}/\sigma_{\rm tot}\simeq 0.17$, as experimentally observed at ISR.

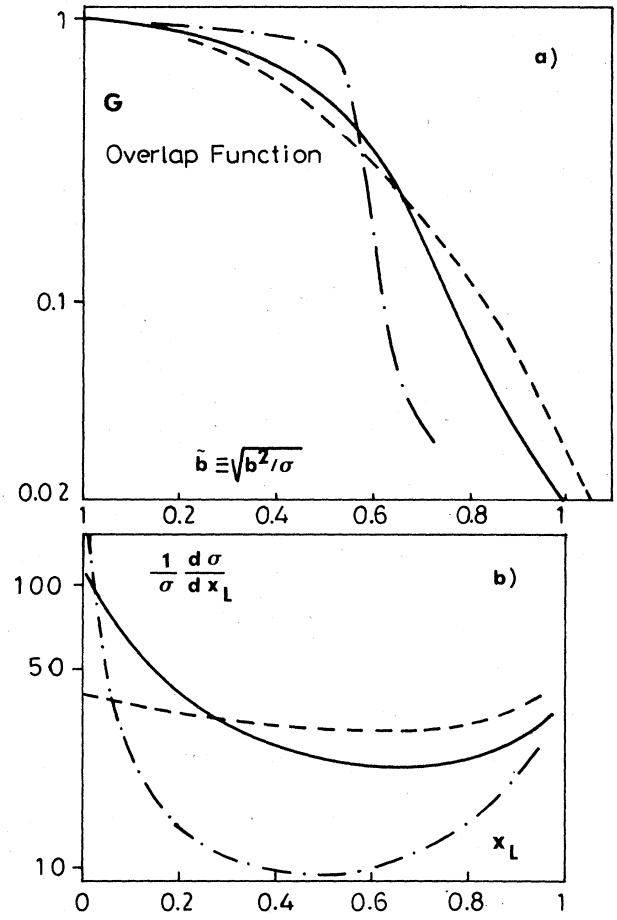

FIG. 2. Predicted correlations between (a) the overlap-function changes and (b) changes in the leading-proton spectrum, Eqs. (6) and (7). The values of $\sigma_{\rm el}/\sigma_{\rm tot}$ are 0.17 (ISR), dashed curve; 0.21 (collider, $\sqrt{s}=540$ GeV), solid curve; 0.28, dashed-dotted curve. The values of $\langle x_L \rangle$ are 0.5, 0.4, and 0.22, respectively.

REMARKS

(i) The leading particle and the leading-proton spectra. The leading proton (or neutron) is not the only leading particle present. The fast hadron jet outside the overlap region produces the proton and also decays in other particles. As the proton is the heaviest stable particle the leading-proton spectrum is the most appropriate to simulate the jet of the leading-particles spectrum. At large x_L the proton spectrum presumably reproduces well the leading-particle spectrum. In the intermediate x_L region,

$0.9 \lesssim x_L \lesssim 0.3$, there are protons which come from $x' > x_L$ jets, but there are jets with $x_L > x''$ which produced protons at lower x''. These effects compensate each other and again the proton spectrum is reasonable. The small x_L region seems the more problematic one: the leading-proton spectrum tends to overestimate the leading-particle spectrum as many of the slow protons come from higher-x leading jets. In conclusion, down to $x_L \simeq 0.2$ the leading-proton spectrum is a reasonable approximation of the leading-particle spectrum.

(ii) Forward-backward correlations. The presence of strong, positive, increasing with energy, forward-backward correlations is one of the most clear predictions of impact-parameter models.[9] The collider data already confirmed such increase, seen also at lower energies, of forward-backward correlations.[10] Finite energy fluctuations in multiplicity and available energy make the simple connections $b^2/\sigma \leftrightarrow n/\langle n \rangle$ and $b^2/\sigma \leftrightarrow x_L$ only true in an average sense. It is then more appropriate, in order to study particle or available energy distributions, to look only at one hemisphere, avoiding the smearing of the fluctuations. At infinite energy there is, of course, no difference as, for the Koba-Nielsen-Olesen distribution functions,

$$\psi(n_B/\langle n_B \rangle) = \psi(n_F/\langle n_F \rangle) = \psi(n/\langle n \rangle) ,$$

and for the available energy fraction distributions $\phi(h_F) = \phi(h_B) = \phi(h)$. Concerning the leading-proton forward-backward correlation, in addition to the finite energy fluctuations, the presence of various leading particles and decaying processes washes away the effect in the intermediate x_L region.[11]

(iii) Determination of available energy. Attempts to estimate directly from SPS $p\bar{p}$ collider data the available energy or inelasticity[1,12] give smaller values than expected from naive application of (1), with $\langle h_A \rangle \simeq 0.3$ (not $\simeq 0.5$). This may indicate that relation (1) is too simple and that some improvement is required. For instance, if one writes instead of (1), $h_A = \alpha G$ with $\alpha \simeq 0.6$, all the arguments presented here remain valid, and the $h_A(b)$ distribution agrees with (1). However, direct determination of h_A may be affected by the presence of neutral particles (either as produced particles or as leading particles) which are not detected. This is particularly true if production of charged particles and production of neutral particles are uncorrelated. On the other hand, the determination of h_A at the SPS $p\bar{p}$ collider may be influenced by the cut in pseudorapidity,[2] $|\eta| < 5$, and the not quite so reasonable approximations, made in calculations, of n independent P_T distributions and production exclusively of pions.

CONCLUSION

Simple geometrical arguments, Eq. (1), lead to the expectation of strong correlations between the shape of the overlap function (and the value of the $\sigma_{\text{el}}/\sigma_{\text{tot}}$ ratio) and the shape of the leading-particle spectrum (Fig. 2). If such correlations turn out not to be experimentally verified, some deeper dynamical argument, as the weakening with energy of the strength of the parton interactions, has to be invoked to explain data (see, for instance, Ref. 13).

ACKNOWLEDGMENTS

I would like to thank P. Kroll, R. Weiner, and G. Wilk for discussions, and the Departments of Physics of the Universities of Bielefeld, Marburg, and Wuppertal for hospitality.

[1] T. T. Chou, Chen Ning Yang, and E. Yen, Phys. Rev. Lett. **54**, 510 (1985).

[2] J. G. Rushbrooke, in *Proceedings of the Fourteenth International Symposium on Multiparticle Dynamics, Lake Tahoe, 1983,* edited by J. F. Gunion and P. M. Yoger (World Scientific, Singapore, 1984).

[3] P. Kroll (private communication); W. Grein, R. Guigas, and P. Kroll, Nucl. Phys. **B89**, 93 (1975); O. Hann, Fortschr. Phys. **27**, 35 (1979).

[4] O. Haan and K. H. Mutter, Phys. Lett. **52B**, 472 (1974).

[5] M. Basile *et al.,* Lett. Nuovo Cimento **38**, 359 (1983).

[6] UA4 Collaboration, M. Bozzo *et al.,* Phys. Lett. **147B**, 392 (1984).

[7] H. Cheng and T. T. Wu, Phys. Rev. Lett. **24**, 1456 (1970); C. Bourrely, J. Soffer, and T. T. Wu, Phys. Rev. D **19**, 3249 (1979); T. T. Chou and C. N. Yang, *ibid.* **19**, 3268 (1979).

[8] UA4 Collaboration, M. Bozzo *et al.,* Phys. Lett. **136B**, 217 (1984).

[9] J. Dias de Deus, Nucl. Phys. **B107**, 146 (1976); T. T. Chou and C. N. Yang, Phys. Lett. **116B**, 301 (1982).

[10] K. Alpgård *et al.,* Phys. Lett. **123B**, 361 (1983).

[11] M. Basile *et al.,* Nuovo Cimento **73A**, 329 (1983).

[12] E. M. Friedlander and R. M. Weiner, Phys. Rev. D **28**, 2903 (1983).

[13] G. N. Fowler, R. M. Weiner, and G. Wilk, Marbourg report, 1984 (unpublished).